Experimental evidence that phosphorus fertilization and arbuscular mycorrhizal symbiosis can reduce the carbon cost of phosphorus uptake

Experimental evidence that phosphorus fertilization and arbuscular mycorrhizal symbiosis can reduce the carbon cost of phosphorus uptake

ARNE VEN[1,2], MELANIE S VERLINDEN[1], ERIK VERBRUGGEN[1], SARA VICCA[1]

[1]*Research Centre of Excellence Plants and Ecosystems, Ecology in a time of change, Univ. of Antwerp, BE-2610 Wilrijk, Belgium*

[2]*correspondence author: Arne.Ven@uantwerpen.be*

I. ABSTRACT

1. Plants allocate substantial amounts of carbon (C) belowground to obtain nutrients and other resources.
2. Increasing nutrient availability typically reduces the C investment in root growth and mycorrhizal fungi, hence reducing the C cost of nutrient acquisition. This C cost of nutrient acquisition, however, remains poorly quantified.
3. In a P fertilization experiment with Zea mays, we examined belowground C allocation and the C cost of phosphorus (P) uptake. In addition, we compared plants inoculated with arbuscular mycorrhizal fungi (AMF) to those growing in pasteurized soil to examine the same measures in the absence of AMF.
4. P fertilization tended to increase aboveground plant growth more than it increased the total belowground C flux (TBCF; root growth plus rhizosphere respiration), suggesting a reduced investment in nutrient acquisition. This was confirmed by a negative fertilization effect on the TBCF-to-total plant P ratio (~25% reduction for high vs low P fertilization). Soil pasteurization increased this proxy for the C cost of P uptake (~50% increase).
5. This novel quantification of the influence of P availability and mycorrhizal fungi on plant-soil C partitioning can guide the incorporation of these processes in vegetation models.

II. KEYWORDS

arbuscular mycorrhizal fungi, phosphorus acquisition, total belowground carbon flux (TBCF), rhizosphere respiration, ^{13}C isotope

III. MAIN TEXT

A. INTRODUCTION

Plants allocate substantial amounts of carbon (C) belowground, among others by growing roots and supporting mycorrhizal fungi to acquire water and nutrients. The fraction of C allocated belowground depends strongly on environmental conditions and especially on the nutrient availability in the soil (e.g. Poorter *et al.*, 2012). When nutrients are scarce, plants typically enhance their belowground C partitioning (i.e., allocation as a fraction of assimilated C) to root growth and activity, and towards mycorrhizal fungi (Fitter, 1991; Richardson, Hocking, Simpson & George, 2009; Tarafdar & Marschner, 1994). In other words, the C cost of nutrient acquisition increases with decreasing nutrient availability (Janssens *et al.*, 2010).

While the inverse relationship between root:shoot ratio and nutrient availability is well-established (Anderson, 1988; Bonifas, Walters, Cassman & Lindquist, 2005; Hammond & White, 2008; Verlinden *et al.*, 2018; Vicca *et al.*, 2012), other aspects of the C investment in nutrient acquisition (e.g. root exudates or mycorrhizal symbiosis) are still poorly quantified. Although soils may contain large nutrient stocks, only a small proportion is easily available to the plants (Richardson *et al.*, 2009; Vicca *et al.*, 2018). Plants can increase their nutrient uptake indirectly through exudation of specific compounds such as phenolics and organic acids that can mobilise insoluble nutrients and stimulate microbial release of nutrients bound to organic matter and minerals (Jones, Hodge & Kuzyakov, 2004; Lambers, Raven, Shaver & Smith, 2008). Alternatively, plants can increase their nutrient uptake directly through symbiosis with microorganisms such as mycorrhizal fungi (Smith & Read, 2008). Compared to plant roots, mycorrhizal fungi have access to a larger portion of soil nutrients because of their large surface-to-volume ratio, and because they produce specific enzymes to release nutrients that are strongly bound to organic matter and minerals (Marschner, 1998; Sanders & Tinker, 1973). As

a result, mycorrhizal fungi can not only consume a considerable fraction of the assimilated C (Hobbie, 2006; Verlinden *et al.*, 2018; Vicca *et al.*, 2012), but can also alter other belowground carbon fluxes (i.e., root respiration, turnover and exudation; Jones *et al.*, 2004; King *et al.*, 2002; Raven, Lambers, Smith & Westoby, 2018). Unravelling the role of mycorrhizal fungi in plant C partitioning patterns is therefore critical to understand ecosystem C cycling and its responses to environmental changes (Heinemeyer *et al.*, 2012; Phillips, Brzostek & Midgley, 2013; Sulman *et al.*, 2017; Terrer, Vicca, Hungate, Phillips & Prentice, 2016; Terrer *et al.*, 2018).

Phosphorus (P) is one of the key limiting elements of plant growth in terrestrial ecosystems (Augusto, Achat, Jonard, Vidal & Ringeval, 2017; Bracken *et al*., 2015; Peñuelas *et al.*, 2013) and symbiosis with arbuscular mycorrhizal fungi (AMF) is a very effective way for plants to acquire scarce and immobile P (Smith & Read, 2008; Smith, Jakobsen, Gronlund & Smith, 2011; Richardson *et al.*, 2009). Moreover, under low P availability, the C cost of P acquisition through AMF and subsequent allocation of C to acquisitive hyphae is expected to be lower than through increased root growth and exudation (Abbott & Robson, 1984; Fitter, 1991; Raven *et al.*, 2018; Treseder, 2013). With increasing P availability, however, the advantage of AMF decreases and a threshold may exist beyond which the C cost of nutrient acquisition through AMF is higher than the cost of P uptake by plant roots (Raven *et al.*, 2018). In such cases, AMF may even negatively influence plant growth (Finlay, 2008; Jones & Smith, 2004; Smith & Smith, 2012).

We set up a mesocosm P fertilization experiment with maize plants (*Zea mays*) and exposed the mesocosms to four different P addition levels to investigate the P addition-effect on belowground C partitioning, including root growth and rhizosphere respiration while also assessing the growth of AMF. We used these data to estimate the C cost of P acquisition in the different treatments. A comparison between plants inoculated with AMF versus plants growing

in pasteurized (and thus AMF-free) soil provided further insight into potential modifications of the C cost of P acquisition by AMF. We hypothesized that P fertilization and presence of AMF decreased belowground C partitioning and reduced the plant C cost of P uptake.

B. MATERIALS AND METHODS

Experimental set-up

The experiment was set up in a greenhouse in Sint-Katelijne-Waver (Belgium, 51°04'38" N, 4°32'05" E) and consisted of 30 mesocosms with insulated walls (1 m × 1.2 m × 0.6 m high), filled with nutrient-poor experimental soil containing C_3 plant derived organic matter (same soil as in Verlinden *et al.*, 2018). The homogenized mixture contained (i) sandy soil (Arenosol) originating from a pine forest in a nature reserve in Belgium with a texture of 95% sand and 5% silt, mixed with (ii) white river sand and (iii) a minor fraction of potting soil in a proportion of 72, 23 and 5 volume %, respectively. The potting soil consisted of a mixture of peat, perlite and fertilizers (NPK 14-16-18, the % of respectively N, P_2O_5 and K_2O; 1.5 kg m^{-3}). The resulting bulk density was 1.379 (± standard error (SE) = 0.006) g cm^{-3}, water saturation was 41.5 (± 0.7) volume %, water field capacity and permanent wilting point were 6.5 (± 0.2) and 0.7 (± 0.1) volume %, respectively. Lime was added to increase the pH of the acidic soil up to an average of 6.19 (± 0.34). This was necessary to stimulate growth of AMF, which is suppressed in sandy soils at pH < 5 (Clark, 2002; Marschener, 1998; van Aarle, Olsson & Soderstrom, 2002).

At the start of the experiment, all mesocosms received a basic level of micronutrients (Fertigreen®, Patentkali® and GroGreen® added in kg ha^{-1}: 79 K, 19 Mg, 53 S, 0.4 B, 0.1 Cu, 2.4 Fe, 1.1 Mn, 0.1 Mo, 0.4 Zn). Since the plants in this experiment are a dwarf type of maize with a mature weight less than half the weight of common maize, we applied only half the P

fertilizer advised for maize crops (i.e., 44.5 kg P_2O_5 ha^{-1}, 50% of the 89 kg P_2O_5 ha^{-1} advised by Roy, Finck, Blair & Tandon, 2006). On 21 June 2017 (i.e. the day of planting), we created a P gradient in 20 mesocosms containing unpasteurized soil by applying 44.5 kg P_2O_5 ha^{-1}s to P4. The other treatments received 12.5, 25 or 50% (P1, P2 and P3, respectively) of the P amount applied in P4. The amounts of P were dissolved as superphosphate (P_2O_5, Janssens-Smeets, Moerdijk, The Netherlands) in water and spread on the soil of each. Since we wanted to create also AMF-free mesocosms to verify indications concerning the role of AMF based on the inoculated treatments, we pasteurized the soil mixture of 10 AMF-free mesocosms by heating them for 4 hours at 80 °C. The 10 pasteurized mesocosms received either the same amount of P as the P1 (P1_noAMF) or the P4 (P4_noAMF) treatments, such that comparisons with pasteurized mesocosms could be made in both the lowest and highest P fertilized treatments. Each treatment consisted of 5 replicate mesocosms.

In summer 2016, the year before the present experiment, the same mesocosms had been used in an N×P experiment. This previous experiment showed that the growth of maize in these soils was strongly limited by P availability, while N was ample as N addition did not affect plant growth (Verlinden *et al.*, 2018). Nonetheless, to ensure that plant growth was not limited by N supply, 95.5 kg N ha^{-1} (calcium nitrate; YaraLiva® Calcinit®, Yara B.V., Rotterdam-Vlaardingen, The Netherlands) was added to each mesocosm on 20 July 2017.

Seeds of *Zea mays* L. (variety ‘Tom Thumb’) were germinated in petri dishes. Fourteen seedlings per mesocosm were planted on June 21st 2017. Before planting, seedlings of the 20 unpasteurized mesocosms were submerged in a pure spore-based inoculum of AMF *Rhizophagus irregularis* (Symplanta®-001 research grade; this 'model AM fungus' often was wrongly named *'Glomus intraradices'* and corresponds to the fungal culture-line known as DAOM197198, DAOM181602 and MUCL43194; 1 million spores, supplied in 250 g water-insoluble fine, humid (50%) diatomite powder). *Rhizophagus irregularis* is a very common

type of AMF, associated with a lot of plants. Seedlings of the 10 pasteurized mesocosms were not inoculated. We did not add a filtrate to the seedlings of the pasteurized mesocosms. Adding a filtrate might have improved the certainty by which differences between the inoculated and pasteurized mesocosms could be attributed to AMF (and not to presence of other soil microorganisms). Future experiments that specifically aim to quantify the influence of removing AMF require addition of a microbial filtrate as well as pasteurization of all soils (i.e., both pasteurized and inoculated) to improve comparability. In our case, we used the pasteurized mesocosms only to strengthen findings concerning the effect of AMF. This provided further insight into potential modifications of the C cost of P acquisition by AMF.

In each mesocosm, soil water content was continuously measured using a reflectometer (CS616, Campbell Scientific, Logan, Utah, USA). To avoid any water stress, we ensured soil water content (SWC) was always between 6 and 12 vol%. Two soil temperature sensors (NTC-WH probe, Carel industries, Manheim, USA) were installed in each mesocosm; soil temperature (°C) at 5 cm depth was logged every 15 minutes for each mesocosm.

Biomass and soil analyses

On 31 August 2017, aboveground and root biomass were harvested for all treatments, except for P1_noAMF where aboveground biomass and root biomass had been harvested 9 days earlier because plants were dying prematurely. Because the harvested biomass clearly underestimated plant growth over the entire season (personal observation of decomposed leaves and presumably also part of the roots), P1_noAMF was not included in the C partitioning analyses (explanation below).

While all of the aboveground biomass was harvested (cut at ~ 1 cm above the soil), root biomass was sampled by taking six cores (7 cm ø, entire soil depth) in each mesocosm. To obtain a spatially representative estimate of root biomass, two of these cores were collected on a stubble (the remainder of the stem after harvest) and the other four at variable distances

between the stubbles. Soil cores were sieved (1 mm mesh) and roots were washed manually. All biomass was oven dried for 72 h at 70 °C before being weighed. Subsamples were ground for further analyses.

For each mesocosm, the $\delta^{13}C$ of the roots was determined on a 2 mg subsample (Elemental Analysis – Isotope Ratio Mass Spectrometry (EA-IRMS) using a CE Instrument EA 1110 elemental analyser, coupled to a Finnigan MAT DeltaPlus IRMS with a Finnigan MAT ConFlo II Interface). The C concentration of different plant parts (roots, leaves, stems, cobs) was determined using an elemental analyser (Flash 2000, Thermo Fisher Scientific, Germany). P and N concentration (g P or N g^{-1} dry biomass) of each plant part was analysed by acid destruction using H_2SO_4, salicylic acid, H_2O_2 and selenium (Walinga, van Vark, Houba & van der Lee, 1989). For each mesocosm, total plant C, N and P contents were calculated from the biomass and C, N and P concentrations of the different plant parts. For each mesocosm, total C contents of aboveground and root biomass were calculated from the biomass and plant part-specific C concentrations.

Soil nutrient availability was assessed using plant root simulator resin probes (PRS™, Western Ag Innovations, Saskatoon, Canada). The probes were inserted into the soil during one week (starting on 13 July 2017) before being analyzed, providing an estimate of the relative availabilities of different nutrients (e.g. Dijkstra *et al.*, 2012; May *et al.*, 2012; Verlinden *et al.*, 2018; Vicca *et al.*, 2018).

AMF measurements

Five mesh bags with C free white river sand (heated for 5 hours at 550 °C to remove any remains of organic matter) which exclude roots but are permeable for fungi (30 µm mesh, size 13 cm × 3 cm × 2 cm, average bulk density 1.37 g cm^{-3}) were buried vertically in the top layer of the soil of each mesocosm one week before planting. They were harvested consecutively, at 11, 33, 47, 61 and 71 days (i.e., at plant harvest) after planting. Hyphae were extracted from 4

g mesh bag sand following the approach of Rillig, Field & Allen (1999; see Appendix S1 in Supporting Information). Hyphal length density (HLD) was calculated as in Rillig *et al.*, 1999 and Tennant, 1975 (see Appendix S1).

Besides hyphal length, we also determined the fatty acid methyl ester (FAME) concentrations, following the protocol of Frostegard, Tunlid & Baath (1993; see Appendix S2 in Supporting Information). The phospholipid fatty acid (PLFA) 16:1ω5 and neutral lipid fatty acid (NLFA) 16:1ω5 were used as indicators for AMF biomass (Olsson, Baath, Jakobsen & Söderström, 1995; Olsson, Francis, Read & Söderström, 1998). NLFA 16:1ω5 is a specific signature compound for AMF, especially when the ratio of NLFA 16:1ω5 to PLFA 16:1ω5 > 1 (Olsson & Johanson, 2000; van Aarle & Olsson, 2003), as was the case in our experiment. PLFA 16:1ω5 can occur in some bacterial groups, but since no PLFA 16:1ω5 could be detected at the start of the experiment and also the pasteurised mesocosms were free of PLFA 16:1ω5, we can assume these PLFAs were primarily AMF-derived (Olsson, Thingstrup, Jakobsen & Baath, 1999; see Table S3 in Supporting Information).

Soil CO_2 fluxes

From the fourth week until the end of the experiment, soil CO_2 efflux and its $\delta^{13}C$ signal were measured weekly in inoculated mesocosms and every two weeks in both inoculated and pasteurized mesocosms, on two types of collars (7.5 cm ø) in each mesocosm. We used a custom-built cuvette (7.5 cm Ø, 16 cm height) coupled to a G2131-i CRDS isotopic-CO_2 gas analyser (Picarro Inc., Santa Clara, CA, USA) operating as a dynamic closed system. One 8 cm high inox collar was pushed 4 cm into the soil before the maize plants were planted, while a 60 cm high PVC collar covered the entire soil depth and thus prevented roots and fungi from growing in. We measured CO_2 effluxes for the different treatments randomly over the course of the day to avoid any potential bias related to the photosynthesis dynamics (Heinemeyer,

Ineson, Ostle & Fitter, 2006). We targeted an increase of the CO_2 concentration inside the cuvette of 100 ppm, which is sufficient to minimize the error on the C source partitioning (Pataki *et al.*, 2003) while also avoiding potential underestimation of CO_2 fluxes due to asymptotic CO_2 flux rates at high CO_2 concentrations (Braendholt, Larsen, Ibrom & Pilegaard, 2017; Kandel, Laerke & Elsegaard, 2016; Kutzbach *et al.*, 2007; Pedersen, Petersen & Schelde, 2010). The CO_2 flux measurements required between 5 and 15 minutes. Given the naturally occurring difference in $\delta^{13}C$ between the C_4 plants and the C_3 soil, these $\delta^{13}C$ flux measurements allowed distinguishing plant-derived C from C originating from the soil organic matter (see Data analyses). Soil moisture inside collars was measured every two weeks, and kept close to field capacity, similar to the surrounding soil.

Plant measurements and leaf area calculation

Biometric, non-destructive plant measurements were made weekly from a plant age of two weeks (3 July 2017) until the end of the experiment. For each mesocosm the amount of surviving plants (n_{plant}) was counted. For at least four plants per mesocosm, the number of living leaves per plant (n_{leaf}) as well as the width (W_{leaf}) and length (L_{leaf}) of each leaf were measured. Individual leaf area (LA) was calculated using the equation of Montgomery (1911):

$$LA = L_{leaf} * W_{leaf} * A_{leaf}, \quad \text{(eq. 1)}$$

with conversion factor $A_{leaf} = 0.75$ for calculating the leaf area of maize (see Montgomery, 1911). Leaf area index (LAI) for each mesocosm was then calculated as:

$$LAI = LA_m\ (cm^2) * n_{plant} * n_{leaf} * (area)^{-1}, \quad \text{(eq. 2)}$$

with LA_m the average LA measured per mesocosm, and n_{plant} and n_{leaf} the number of plants and leaves, respectively. The surface area (area) of each mesocosm was $1.2 * 10^4$ cm^2. Average LAI was calculated for each treatment. Pictures were taken four times a week from 150 cm above the canopy to determine the time of growth initiation of cobs and ears in each mesocosm.

232 ***Data analyses***

233 We calculated rhizosphere respiration (R_{rhizo}) using the CO_2 effluxes and associated $\delta^{13}C$ from
234 the two collars installed in each mesocosm. The soil CO_2 efflux from the open inox collar (R_{soil})
235 is the sum of soil organic matter decomposition (SOM_{dec}) and R_{rhizo}. The soil CO_2 efflux from
236 the PVC collar comprises only the decomposition of the organic matter (R_{SOM}; in the absence
237 of roots and AMF). This collar was used to determine the $\delta^{13}C$ of organic matter decomposition
238 ($\delta^{13}C$ R_{SOM}) necessary for the partitioning of R_{soil} into SOM_{dec} and R_{rhizo}. For this partitioning,
239 we applied a basic mixing equation (Balesdent, Mariotti & Guillet, 1987), using $\delta^{13}C$ R_{SOM} and
240 the $\delta^{13}C$ of the roots as end-members:

241 $$f_{rhizo} = (\delta^{13}C\ R_{soil} - \delta^{13}C\ R_{SOM}) * (\delta^{13}C\ roots - \delta^{13}C\ R_{SOM})^{-1}, \quad \text{(eq. 3)}$$

242 with f_{rhizo} the rhizosphere respiration as a fraction of R_{soil}. R_{rhizo} is then calculated as:

243 $$R_{rhizo} = f_{rhizo} * R_{soil}. \quad \text{(eq. 4)}$$

244 To avoid confounding effects of varying temperatures in the comparison among treatments, we
245 computed for each measurement period the basal rate of R_{rhizo} (R_{25}), i.e., the flux rate at 25 °C
246 (this was approximately the median temperature over all periods used in our analyses). To this
247 end, we fitted equation 6 to the data:

248 $$R_{rhizo} = R_{25} * Q_{10}^{(T - 25) / 10}, \quad \text{(eq. 5)}$$

249 where Q_{10} represents the temporal temperature sensitivity (Davidson & Janssens, 2006; Vicca
250 *et al.*, 2009) and T is the soil temperature (°C) at 5 cm depth.
251 Rhizosphere respiration varied over the season, depending on both plant development and soil
252 temperature. To estimate total R_{rhizo} ($\sum R_{rhizo}$) over the entire growing season, we extrapolated
253 R_{rhizo} over time using a time- and temperature-dependent regression function fitted for each
254 treatment separately. Because soil measurements with the isotope laser started only on 17 July
255 2017, we added R_{rhizo} = 0 for the day of planting (21 June 2017) to the dataset (this hardly

affected the fit results and $\sum R_{rhizo}$ (see Table S4 in Supporting Information)). Specifically, we fitted the following equation to the R_{rhizo} data of each treatment:

$$\log_{10}(\text{observed } R_{rhizo}+1) = a + b * T_t + c * t^2 + d * t, \quad \text{(eq. 6)}$$

where a, b, c and d are the estimated coefficients of the observed R_{rhizo} and T_t is T at 5 cm depth at time t. Comparison of predicted and observed R_{rhizo} indicates that the regression model captured the patterns for each treatment fairly well, as R^2 for predicted versus observed R_{rhizo} ranged between 0.25 and 0.51 (see Fig. S5 in Supporting Information).

Belowground C partitioning and its response to P addition and mycorrhization was investigated by expressing root biomass C (BP_{root}) and $\sum R_{rhizo}$ relative to aboveground biomass production (BP_{above}) (i.e., using the root:shoot ratio and the $\sum R_{rhizo}$:BP_{above} ratio). We also calculated total belowground carbon flux (TBCF) as the sum of BP_{root} and $\sum R_{rhizo}$. Although this calculation does not explicitly include root exudation and mycorrhizal biomass, we assume that turnover of both is fast (more or less 30 days for AMF; Ekblad *et al.*, 2016; Olsson & Johnson, 2005) and is thus at least partly captured by R_{rhizo}. Nonetheless, we acknowledge that TBCF as calculated here presents a slight underestimation, but we consider this negligible for the objectives of this study, where TBCF serves primarily for comparison of belowground C partitioning among treatments (i.e., TBCF:BP_{above}). Last, we used TBCF:$P_{tot,}$ (with P_{tot} being the total plant P content), as a proxy for the C cost of P acquisition for testing the response of this C cost to increasing P availability and to mycorrhization (similar to Terrer *et al.*, 2018, where fine-root production, fine-root biomass or root biomass relative to the total plant N content (N_{tot}) was used as a proxy for the C cost of N acquisition). This approximation is based on the premise that under P-limited conditions, plants increase their investment in root growth and activity (including exudation and C allocation to AMF) with decreasing P availability (Raven *et al.*, 2018). Hence, a P fertilization effect on TBCF:P_{tot} is assumed to reflect the change in the C cost of P uptake.

281 ***Statistical analyses***

282 All statistical analyses were performed in R (RStudio Team, 2016). To ensure robust estimates
283 of belowground C partitioning (expressing BP_{root}, $\sum R_{rhizo}$ and TBCF relative to BP_{above}), outlier
284 mesocosms for BP_{above} within each treatment were removed from all analyses (we applied the
285 extreme studentized deviate (ESD) test, which detected one outlier in P2). Data normality of
286 residuals was checked using the Shapiro-Wilk test. A Principal Component Analysis (PCA)
287 was performed for a general visualization of the link among the dependent variables across the
288 treatments (see Fig. S6 in Supporting Information). Analyses of covariance (ANCOVA) were
289 applied using treatment as a continuous numeric variable (i.e., 2.5, 5, 10 and 20 kg P ha^{-1}) to
290 test if BP_{above}, BP_{root}, TBCF, and TBCF:P_{tot} changed with increasing P addition in inoculated
291 mesocosms. For in-depth understanding of changes in belowground C partitioning, the same
292 test was also done on a selection of C partitioning-related parameters, more specifically on the
293 root:shoot ratio, PLFA 16:1ω5, $\sum R_{rhizo}$:BP_{above}, $\sum R_{rhizo}$:BP_{root}, TBCF:BP_{above}, P_{tot} and N_{tot} (i.e.
294 respectively the total plant P and N content), the N:P ratio, the PRS™-probe nutrient supply
295 rates, leaf N content and leaf P content. A non-parametric Mann-Whitney U test (in R using
296 the code wilcox.test) using only P4 and P4_noAMF was applied to test the pasteurization
297 effect. $\sum R_{rhizo}$ was computed as one value per treatment (not per mesocosm), presenting the
298 average cumulated value of the total growing season. For each treatment, $\sum R_{rhizo}$ was thus
299 represented by one value with a standard error. Therefore, these data were analysed with a
300 weight variable, inversely proportional to the standard error. A linear model was fitted to verify
301 the effect of P fertilization level (2.5, 5, 10 and 20 kg P ha^{-1}) on $\sum R_{rhizo}$ in inoculated
302 mesocosms. The significance of the pasteurization effect on $\sum R_{rhizo}$ was estimated using a t-
303 test based on the difference between P4 and P4_noAMF, divided by their common SE. An
304 ANCOVA with time as a covariate was applied to test if LAI, R_{25} and HLD changed over time

and differed among treatments (which were included as fixed factors), taking into account interactions between treatment and time or time^2.

C. RESULTS

The fertilizer application produced a gradient of P availability while N availability was high in all mesocosms (Table 1). P fertilization increased both above- and belowground plant growth and their total C, P and N content (Table 1, Fig. S6), with BP_{above}, P_{tot} and N_{tot} being about four times higher in P4 than in P1, and approximately a doubling of BP_{root} from P1 to P4. The N:P ratio slightly decreased with increasing P fertilization (Table 1). The belowground plant C pools and fluxes, i.e., $\sum R_{rhizo}$, TBCF and PLFA 16:1ω5 (indicative of AMF biomass), significantly increased with increasing P fertilization (Fig. 1**a**, **b**, **c**). The P fertilization effects on biomass and nutrient contents were especially pronounced for P1 and P2 versus P3 and P4. Pasteurization (which was successful since no AMF hyphae were found in P4_noAMF, Fig. 4**c**) reduced the presence of AMF to zero (Fig. 1**c**) and significantly reduced the total plant C, N and P content; BP_{above}, BP_{root}, N_{tot} and P_{tot} decreased by at least 50%. The N:P ratio was significantly higher in P4_noAMF than in P4 (Table 1). The belowground plant C fluxes ($\sum R_{rhizo}$ and TBCF) decreased by more than 50% in P4_noAMF relative to P4 (Fig. 1**a, b**).

The effect of P fertilization and pasteurization on C partitioning to belowground pools and fluxes, and ultimately on the C cost of P acquisition, was examined by comparing the plant C pools and fluxes relative to BP_{above}, BP_{root} and P_{tot}. The root:shoot ratio significantly decreased with increasing P fertilization, but was not affected by pasteurization (Table 1). On the other hand, $\sum R_{rhizo}$:BP_{above} was not affected by P fertilization but was significantly lower in the pasteurized soil (Fig. 2**a**). As a consequence, the partitioning to TBCF (i.e., the sum of BP_{root} and $\sum R_{rhizo}$ relative to BP_{above}) slightly decreased with increasing P fertilization ($p = 0.08$ for

329 the P effect on TBCF:BP_{above}; Fig. 2**c**). Pasteurization significantly reduced TBCF:BP_{above} from
330 approximately 0.49 g g^{-1} C in P4 to 0.37 g g^{-1} in P4_noAMF (Fig. 2**c**). Interestingly,
331 $\sum R_{rhizo}$:BP_{root}, which is indicative for the relative investment of plants in rhizosphere activity
332 (root respiration, exudation and mycorrhizal activity) versus root growth, increased with P
333 fertilization and was reduced by pasteurization (Fig. 2**b**). Overall, P fertilization seemed to
334 decrease the C cost of P acquisition, given the significantly negative effect on the TBCF:P_{tot}
335 ratio (~25% reduction in P3 and P4 relative to P1 and P2; Fig. 3). Pasteurization had a
336 significantly positive effect on this proxy for the C cost of P acquisition, with TBCF:P_{tot} in
337 P4_noAMF approximately 50% higher than in P4 (Fig. 3).
338 The P fertilization effect on plant growth, rhizosphere respiration and AMF varied over the
339 course of the season (significant P fertilization × time interaction effect for LAI, R_{25} and HLD;
340 Fig. 4**a**, **b**, **c**). LAI increased over time as plants grew (until about 50 days after planting), and
341 this increase over time was stronger for the P fertilized treatments (Fig. 4**a**). For R_{25}, we
342 observed a linear increase over time in P1 and P2, while P3 and P4 showed an initial increase
343 but decreased again towards the end of the growing season (Fig. 4**b**). HLD increased over time,
344 with P1 and P2 following a log-linear curve, while P3 and P4 showed a log-linear increase until
345 about 7 weeks after planting, when HLD decreased again. Also pasteurization affected the time
346 course of LAI and R_{25}; in P4_noAMF, LAI increased with time at a similar rate as in P4 until
347 ca. 30 days after planting, after which it levelled off and decreased (Fig 4**a**). Pasteurization
348 negatively affected R_{rhizo}, as in P4_noAMF R_{25} was more than 50% smaller than that in P4
349 during the entire measurement period (Fig. 4**b**). R_{25} in P4 increased until a maximum was
350 reached at ca. 47 days after planting after which it decreased again. In contrast, P4_noAMF
351 showed a linear (borderline significant) increase over time, as reflected in the significant time
352 interaction effect (Fig. 4**b**).
353

D. DISCUSSION

Low P availability clearly limited plant growth in our experiment. Associated with the biomass increases, also TBCF increased with increasing P fertilization, but, as expected, this increase was smaller than the increase in BP_{above} (i.e., TBCF relative to BP_{above} decreased). This reduction in belowground C partitioning indicates a reduced need of the plants to invest in nutrient acquisition when P was added. The negative P fertilization effect on belowground C partitioning reflected primarily a reduced partitioning to root growth (root:shoot ratio decreased), as partitioning to rhizosphere respiration ($\sum R_{rhizo}$:BP_{above}) was not significantly affected by P fertilization.

Interestingly, $\sum R_{rhizo}$:BP_{root} increased with P fertilization, indicating enhanced C losses per unit root biomass. These C losses may reflect increased mass-specific root respiration, increased mycorrhizal carbon use per unit root biomass, and/or increased release of exudates that are rapidly consumed by the rhizosphere microbes. At first sight, the increased $\sum R_{rhizo}$:BP_{root} may suggest reduced efficiency of resource uptake by the roots,. However, TBCF:P_{tot} decreased by about 40% (P4 vs P1), indicating a decrease of the total C cost of P uptake. In other words, the increased return on investment under P fertilization more than compensated for the increased C losses per unit root biomass. Apparently, the plant strategy for P uptake changed over the P gradient, with increasing P stimulating C investment in rhizosphere processes other than root growth that are more efficient for P uptake. The increasing AMF hyphal growth with increasing P availability suggests a key role for the AMF in this response.

In our experiment, we included also two pasteurized treatments, i.e., where no AMF were present. Although pasteurization may also have altered the amount and composition of soil microbes other than AMF, which may have contributed to the pasteurization effect on belowground C fluxes, the comparison between P4 and P4_no AMF provides interesting support for the role of AMF in plant C partitioning and C uptake. Pasteurization decreased

379 belowground C partitioning (as reflected in TBCF:BP_{above} and $\sum R_{rhizo}$:BP_{above}), but increased
380 TBCF:P_{tot}, which was about 50% lower in P4 than in P4_noAMF. Hence, pasteurization
381 reduced the amount of C respired per unit root, but the return on investment was reduced more
382 as reflected in the increased C cost of P acquisition. Although future studies where all soils are
383 initially pasteurized and only part is inoculated with AMF are needed to rule out any
384 contribution of potential microbial shifts to the observed pasteurization effect, these results
385 provide strong support for a role of AMF in explaining the higher $\sum R_{rhizo}$:BP_{root} but lower C
386 cost of P uptake with increasing P fertilization in the inoculated mesocosms.
387 Both the P gradient in the inoculated mesocosms and the comparison of P4 and P4_noAMF
388 indicated that AMF symbiosis was the most efficient pathway for plants to acquire P, even
389 under high P availability. This is in contrast with the expectation that at high P availability, P
390 uptake via AMF is more expensive in comparison with uptake via roots due to costs of transport
391 through hyphae (Raven *et al.*, 2018). Possibly, relative costs of root versus mycorrhizal P
392 uptake is specific to plant species such as maize that are very nutrient-demanding and highly
393 dependent on AMF (Hartnett & Wilson, 1999; Hoeksema *et al.*, 2010; Wilson & Hartnett,
394 1998). The extent to which our findings can be generalized to other species and ecosystems
395 needs further testing. With our experiment we demonstrate how stable isotope methods can be
396 used to quantify the C cost of nutrient acquisition. This method can also be used for other plant
397 species, for example by growing C_3 plants on a C_4 soil (Kuzyakov, 2006).
398 Besides a clear effect of P fertilization and pasteurization, plant C partitioning also varied over
399 the course of the growing season, as temporal patterns of LAI (as an indication of leaf growth)
400 differed from patterns of R_{25} (a temperature-independent estimate of rhizosphere respiration)
401 and HLD (an estimate of AMF growth). As nutrient requirements depend on plant growth and
402 developmental stage, belowground C partitioning indeed is expected to vary over time because
403 of changing needs during e.g. plant growth and flower or fruit production (Gransee &

Wittenmayer, 2000; Litton, Raich & Ryan, 2007; Liu *et al.*, 2018; Yu, Li, Jin, Liu & Wang, 2017). Leaves, roots and AMF increased in biomass until about 47 days after planting, which was approximately the starting time of fruit (cob) ripening. At this time, C partitioning to leaves decreased, as indicated by the flattening of the LAI increase. Under high P fertilization (P3 and P4), also C partitioning to rhizosphere (R_{25}) tended to decrease at this time of the season, suggesting a decrease in root and AMF activity. The reduced belowground C partitioning towards the end of the season under high P availability was reflected also in the hyphal growth since HLD decreased when cobs started ripening. This indicates that, towards the end of the season, hyphal decomposition exceeded hyphal growth. Similar patterns were also observed in an experiment with *Plantago lanceolata* (Olsson & Johnson, 2005). These results are in line with earlier research on belowground C allocation, where young plants were found to produce higher amounts of root exudates per gram of root dry matter and to allocate more C to roots and soil than older plants (Gransee & Wittenmayer, 2000; Yu *et al.*, 2017), probably because at an early growth stage the demand for nutrients is highest (Schilling, Gransee, Deuhel, Lezoviz & Ruppel, 1998). However, in our experiment R_{25} and HLD did not decrease upon cob ripening for the two treatments with low P availability (P1 and P2). This suggests that plants in P1 and P2 were still in a growth phase where they invested in AMF to acquire P needed for cob ripening (note that cobs had the highest P concentration of all plant parts; see Table S7 in Supporting Information). Hence, under low nutrient availability, the demand for nutrients can still be high at plant maturity.

Our experiment demonstrated that P fertilization strongly reduced total belowground C partitioning as well as the C cost of P acquisition. Our results provide interesting support for the role of AMF in plant C partitioning and C uptake, and suggest that AMF symbiosis was the most efficient pathway for P uptake, even at high P availability. These findings provide

fundamental insights that can also guide the incorporation of P availability and mycorrhizal fungi in vegetation models.

IV. ACKNOWLEDGEMENTS

This research was supported by the Research Foundation – Flanders (FWO) G0D5415N, by the European Research Council grant ERC-SyG-610028 IMBALANCE-P, ClimMani COST Action (ES1308) and by Methusalem funding of the Research Council UA. We acknowledge Fred Kockelbergh and Marc Wellens for technical support, Bart Hellemans, Lin Leemans and Eddy De Smet for logistic support at the field site, Janset Namli for help with fieldwork, Miguel Portillo Estrada for laboratory analyses, Erik Fransen for statistical advice, and Pål Axel Olsson for advice, scientific discussions and laboratory analyses. We gratefully thank the Isotope bioscience laboratory (ISOFYS) of Ghent University for lending their Picarro G2131-i CRDS isotopic-CO_2 gas analyser.

V. AUTHORS' CONTRIBUTIONS

SV designed the research; AV and MV conducted the field- and lab work; AV drafted the paper; and AV, MV, EV and SV contributed to the interpretation of the results and to the writing of the paper.

VI. DATA AVAILABILITY STATEMENT

Data can be found in Zenodo (Ven *et al*., 2019): doi.org/10.5281/zenodo.3387198

VII. REFERENCES

Abbott, L.K., & Robson, A.D. (1984). Formation of external hyphae in soil by 4 species of vesicular arbuscular mycorrhizal fungi. *New Phytologist*, 99(2), 245–255. doi: 10.1111/j.1469-8137.1985.tb03653.x

Anderson, E.L. (1988). Tillage and N-fertilization effects on maize root-growth and root-shoot ratio. *Plant and Soil*, 108(2), 245–251. doi: 10.1007/BF02375655

Augusto, L., Achat, D.L., Jonard, M., Vidal, D., & Ringeval, B. (2017). Soil parent material – a major driver of plant nutrient limitations in terrestrial ecosystems. *Global Change Biology*, 23(9), 3808–3824. doi: 10.1111/gcb.13691

Balesdent, J., Mariotti, A., & Guillet, B. (1987). Natural C-13 abundance as a tracer for studies of soil organic matter dynamics. *Soil Biology & Biochemistry*, 19(1), 25–30. doi: 10.1016/0038-0717(87)90120-9

Bonifas, K.D., Walters, D.T., Cassman, K.G., & Lindquist, J.L. (2005). Nitrogen supply affects root:shoot ratio in corn and velvetleaf (*Abutilon theophrasti*). *Weed Science*, 53(5), 670–675. doi: 10.1614/WS-05-002R.1

Bracken, M.E.S., Hillebrand, H., Borer, E.T., Seabloom, E.W., Cebrian, J., Cleland, E.E., … Smith, J.E. (2015). Signatures of nutrient limitation and co-limitation: Responses of autotroph internal nutrient concentrations to nitrogen and phosphorus additions. *Oikos*, 124(2), 113–121. doi: 10.1111/oik.01215

Braendholt, A., Larsen, K.S., Ibrom, A., & Pilegaard, K. (2017). Overestimation of closed-chamber soil CO_2 effluxes at low atmospheric turbulence. *Biogeosciences*, 14(6), 1603-1616. doi: 10.5194/bg-14-1603-2017

472 **Clark, D.A. (2002).** Are tropical forests an important carbon sink? Reanalysis of the long-term
473 plot data. *Ecological Applications*, 12(1), 3–7. doi: 10.1890/1051-
474 0761(2002)012[0003:ATFAIC]2.0.CO;2
475 **Davidson, E.A., & Janssens, I.A. (2006).** Temperature sensitivity of soil carbon
476 decomposition and feedbacks to climate change. *Nature*, 440(9), 165–173. doi:
477 10.1038/nature04514
478 **Dijkstra, F.A., Pendall, E., Morgan, J.A., Blumenthal, D.M., Carrillo, Y., LeCain, D.R.,**
479 **… Williams, D.G. (2012).** Climate change alters stoichiometry of phosphorus and nitrogen in
480 a semiarid grassland. *New Phytologist*, 196(3), 807–815. doi: 10.1111/j.1469-
481 8137.2012.04349.x.
482 **Ekblad, A., Mikusinska, A., Agren, G.I., Menichetti, L., Wallander, H., Vilgalys, R., …**
483 **Eriksson, U. (2016).** Production and turnover of ectomycorrhizal extrametrical mycelial
484 biomass and necromass under elevated CO2 and nitrogen fertilization. *New Phytologist*,
485 211(3), 874–885. doi: 10.1111/nph.13961
486 **Finlay, R.D. (2008).** Ecological aspects of mycorrhizal symbiosis: with special emphasis on
487 the functional diversity of interactions involving the extraradical mycelium. *Journal of*
488 *Experimental Botany*, 59(5), 1115–1126. doi: 10.1093/jxb/ern059
489 **Fitter, A.H. (1991).** Costs and benefits of mycorrhizas: Implications for functioning under
490 natural conditions. Experientia, 47(4), 350–355.
491 **Frostegard, A., Tunlid, A., & Baath, E. (1993).** Phospholipid fatty-acid composition,
492 biomass, and activity of microbial communities from 2 soil types experimentally exposed to
493 different heavy-metals. *Applied and Environmental Microbiology*, 59(11), 3605–3617.
494 **Gransee, A., & Wittenmayer, L. (2000).** Qualitative and quantitative analysis of water-
495 soluble root exudates in relation to plant species and development. *Journal of Plant Nutrition*
496 *and Soil Science*, 163(4), 381–385. doi: 10.1002/1522-2624(200008)163

Hammond, J.P., & White, P.J. (2008). Sucrose transport in the phloem: integrating root responses to phosphorus starvation. *Journal of Experimental Botany*, 59(1), 93–109. doi: 10.1093/jxb/erm221

Hartnett, D.C., & Wilson, G.W.T. (1999). Mycorrhizae influence plant community structure and diversity in tallgrass prairie. *Ecology*, 80(4), 1187–1195. doi: 10.1890/0012-9658(1999)080

Heinemeyer, A., Ineson, P., Ostle, N., Fitter, A.H. (2006). Respiration of the external mycelium in the arbuscular mycorrhizal symbiosis shows strong dependence on recent photosynthates and acclimation to temperature. *New Phytologist*, 171, 159-170.

Heinemeyer, A., Wilkinson, M., Vargas, R., Subke, J.-A., Casella, E., Morison, J.I.L., & Ineson, P. (2012). Exploring the "overflow tap" theory: linking forest soil CO2 fluxes and individual mycorrhizosphere components to photosynthesis. *Biogeosciences*, 9, 79-95. doi: 10.5194/bg-9-79-2012

Hobbie, E.A. (2006). Carbon allocation to ectomycorrhizal fungi correlates with belowground allocation in culture studies. *Ecology*, 87(3), 563–569.

Hoeksema, J.D., Chaudhary, V.B., Gehring, C.A., Johnson, N.C., Karst, J., Koide, R.T., ... Umbanhowar, J. (2010). A meta-analysis of context-dependency in plant response to inoculation with mycorrhizal fungi. *Ecology Letters*, 13(3), 394–407. doi: 10.1111/j.1461-0248.2009.01430.x.

Janssens, I.A., Dieleman, W., Luyssaert, S., Subke, J.A., Reichstein, M., Ceulemans, R., ... Law, B.E. (2010). Reduction of forest soil respiration in response to nitrogen deposition. *Nature Geoscience*, 3(5), 315–322. doi: 10.1038/ngeo844

Jones, D.L., Hodge, A., & Kuzyakov, Y. (2004). Plant and mycorrhizal regulation of rhizodeposition. *New Phytologist*, 163(3), 459–480. doi: 10.1111/j.1469-8137.2004.01130.x

521 **Jones, M.D., & Smith, S.E. (2004).** Exploring functional definitions of mycorrhizas: Are
522 mycorrhizas always mutualisms? *Canadian Journal of Botany*, 82(8), 1089–1109. doi:
523 10.1139/b04-110
524 **Kandel, T.P., Laerke, P.E., & Elsegaard, L. (2016).** Effect of chamber enclosure time on soil
525 respiration flux: A comparison of linear and non-linear flux calculation methods. *Atmospheric*
526 *Environment*, 141, 245-254. doi: 10.1016/j.atmosenv.2016.06.062
527 **King, J.S., Albaugh, T.J., Allen, H.L., Buford, M., Strain, B.R., & Dougherty, P. (2002).**
528 Below-ground carbon input to soil is controlled by nutrient availability and fine root dynamics
529 in loblolly pine. *New Phytologist*, 154(2), 389–398.
530 **Kutzbach, L., Schneider, J., Sachs, T., Giebels, M., Nykänen, H., Shulpali, N.J., …**
531 **Wilmking, M. (2007).** CO_2 flux determination by closed-chamber methods can be seriously
532 biased by inappropriate application of linear regression. *Biogeosciences*, 4, 1005–1025. doi:
533 10.5194/bg-4-1005-2007
534 **Kuzyakov, Y. (2006).** Sources of CO_2 efflux from soil and review of partitioning methods.
535 *Soil Biology & Biochemistry*, 38, 425-448. doi: 10.1016/j.soilbio.2005.08.020
536 **Lambers, H., Raven, J.A., Shaver, G.R., & Smith, S.E. (2008).** Plant nutrient-acquisition
537 strategies change with soil age. *Trends in Ecology & Evolution*, 23(2), 95–103. doi:
538 10.1016/j.tree.2007.10.008.
539 **Litton, C.M., Raich, J.W., & Ryan, M.G. (2007).** Carbon allocation in forest ecosystems.
540 *Global Change Biology*, 13(10), 2089–2109. doi: 10.1111/j.1365-2486.2007.01420.x
541 **Liu, S.J., Guo, H.L., Xu, J., Song, Z.Y., Song, S.R., Tang, J.J., & Chen, X. (2018).**
542 Arbuscular mycorrhizal fungi differ in affecting the flowering of a host plant under two soil
543 phosphorus conditions. *Journal of Plant Ecology*, 11(4), 623–631. doi: 10.1093/jpe/rtx038

544 **Marschener, H. (1998).** Role of root growth, arbuscular mycorrhiza, and root exudates for the
545 efficiency in nutrient acquisition. *Field Crops Research*, 56(1-2), 203–207. doi:
546 10.1016/S0378-4290(97)00131-7

547 **May, W.E., Malhi, S.S., Holzapfel, C.B., Nybo, B.X., Schoenau, J., & Lafond, G.P. (2012).**
548 The effects of chloride and potassium nutrition on seed yield of annual canarygrass. *Agronomy*
549 *Journal*, 104(4), 1023–1031. doi: 10.2134/agronj2011.0414

550 **Montgomery, E.G. (1911).** "*Correlation studies in corn", 24th Annual Report, Agricultural*
551 *Experiment Station*. Nebraska, Mo, USA.

552 **Olsson, P.A., Baath, E., Jakobsen, I., & Söderström, B. (1995).** The use of phospholipid
553 and neutral lipid fatty acids to estimate biomass of arbuscular mycorrhizal fungi in soil.
554 *Mycological Research*, 99(5), 623–629. doi: 10.1016/S0953-7562(09)80723-5

555 **Olsson, P.A., Francis, R., Read, D.J., & Soderstrom, B. (1998).** Growth of arbuscular
556 mycorrhizal mycelium in calcareous dune sand and its interaction with other soil
557 microorganisms as estimated by measurement of specific fatty acids. *Plant and Soil*, 201(1),
558 9–16. doi: 10.1023/A:1004379404220

559 **Olsson, P.A., Thingstrup, I., Jakobsen, I., & Baath, E. (1999).** Estimation of the biomass of
560 arbuscular mycorrhizal fungi in a linseed field. *Soil Biology & Biochemistry*, 31(13), 1879–
561 1887. doi: 10.1016/S0038-0717(99)00119-4

562 **Olsson, P.A., & Johanson, A. (2000).** Lipid and fatty acid composition of hyphae and spores
563 of arbuscular mycorrhizal fungi at different growth stages. *Mycological Research*, 104(4), 429–
564 434. doi: 10.1017/S0953756299001410

565 **Olsson, P.A., & Johnson, N.C. (2005).** Tracking carbon from the atmosphere to the
566 rhizosphere. *Ecology Letters*, 8(12), 1264–1270. doi: 10.1111/j.1461-0248.2005.00831.x

Pataki, D.E., Ehleringer, J.R., Flanagan, L.B., Yakir, D., Bowling, D.R., Still, C.J., … Berry, J.A. (2003). The application and interpretation of Keeling plots in terrestrial carbon cycle research. *Global Biogeochemical Cycles*, 17(1), 1-14. doi: 10.1029/2001GB001850

Pedersen, A.R., Petersen, S.O., & Schelde, K. (2010). A comprehensive approach to soil-atmosphere trace-gas flux estimation with static chambers. *European Journal of Soil Science*, 61(6), 888-902. doi: 10.1111/j.1365-2389.2010.01291.x

Peñuelas, J., Poulter, B., Sardans, J., Ciais, P., van der Velde, M., Bopp, L., … Janssens, I.A. (2013). Human-induced nitrogen-phosphorus imbalances alter natura land managed ecosystems across the globe. *Nature Communications*, 4, 1–10. doi: 10.1038/ncomms3934

Phillips, R.P., Brzostek, E., & Midgley, M.G. (2013). The mycorrhizal associated nutrient economy: a new framework for predicting carbon nutrient couplings in temperate forests. *New Phytologist*, 199(1), 41–51. doi: 10.1111/nph.12221

Poorter, H., Niklas, K.J., Reich, P.B., Oleksyn, J., Poot, P., & Mommer, L. (2012). Biomass allocation to leaves, stems and roots: meta-analyses of interspecific variation and environmental control. *New Phytologist*, 193(1), 30–50. doi: 10.1111/j.1469-8137.2011.03952.x

Raven, J.A., Lambers, H., Smith, S.E., & Westoby, M. (2018). Costs of acquiring phosphorus by vascular land plants: patterns and implications for plant coexistence. *New Phytologist*, 217(4), 1420–1427. doi: 10.1111/nph.14967

Richardson, A.E., Hocking, P.J., Simpson, R.J., & George, T.S. (2009). Plant mechanisms to optimise access to soil phosphorus. *Crop & Pasture Science*, 60(2), 124–143. doi: 10.1071/CP07125

Rillig, M.C., Field, C.B., & Allen, M.F. (1999). Soil biota responses to long-term atmospheric CO2 enrichment in two California annual grasslands. *Oecologia*, 119(4), 572–577. doi: 10.1007/s004420050821

592 **Roy, R.N., Finck, A., Blair, G.J., & Tandon, H.L.S. (2006).** Plant nutrition for food security:
593 A guide for integrated nutrient management. Food and Agriculture Organization of the United
594 Nations (FAO), Rome.
595 **RStudio Team. 2016.** RStudio: Integrated Development for R. RStudio, Inc., Boston, MA
596 URL http://www.rstudio.com/.
597 **Sanders, E.S., & Tinker, P.B. (1973).** Phosphate flow into mycorrhizal roots. *Pest*
598 *Management Science*, 4(3), 385–395. doi: 10.1002/ps.2780040316
599 **Schilling, G., Gransee, A., Deuhel, A., Lezoviz, G., & Ruppel, S. (1998).** Phosphorus
600 availability, root exudates, and microbial activity in the rhizosphere. *Journal of Plant Nutrition*
601 *and Soil Science*, 161(4), 333–484. doi: 10.1002/jpln.1998.3581610413
602 **Smith, S.E., & Read, D.J. (2008).** *Mycorrhizal symbiosis*. London, UK: Academic Press and
603 Elsevier.
604 **Smith, S.E., Jakobsen, I., Gronlund, M., & Smith, F.A. (2011).** Roles of arbuscular
605 mycorrhizas in plant phosphorus nutrition: interactions between pathways of phosphorus
606 uptake in arbuscular mycorrhizal roots have important implications for understanding and
607 manipulating plant phosphorus acquisition. *Plant Physiology*, 156(3), 1050–1057. doi:
608 10.1104/pp.111.174581
609 **Smith, S.E., & Smith, F.A. (2012).** Fresh perspectives on the roles in arbuscular mycorrhizal
610 fungi in plant nutrition and growth. *Mycologia*, 104 (1), 1–13. doi: 10.3852/11-229
611 **Sulman, B.N., Brzostek, E.R., Medici, C., Shevliakova, E., Menge, D.N.L., & Philips, R.B.**
612 **(2017).** Feedbacks between plant N demand and rhizosphere priming depend on type of
613 mycorrhizal association. *Ecology Letters*, 20(8), 1043–1053. doi: 10.1111/ele.12802
614 **Tarafdar, J.C., & Marschner, H. (1994).** Efficiency of VAM hyphae in utilization of organic
615 phosphorus by wheat plants. *Soil Science and Plant Nutrition*, 40(4), 593–600. doi:
616 10.1080/00380768.1994.10414298

Tennant, D. (1975). A test of a modified line intersect method of estimating root length. *The Journal of Ecology*, 63(3), 995–1001.

Terrer, C., Vicca, S., Hungate, B.A., Phillips, R.P., & Prentice, I.C. (2016). Mycorrhizal association as a primary control of the CO2 fertilization effect. *Science*, 353(6294), 72–74. doi: 10.1126/science.aaf4610

Terrer, C., Vicca, S., Stocker, B.D., Hungate, B.A., Phillips, R.P., Reich, P.B., … Prentice, I.C. (2018). Ecosystem responses to elevated CO2 governed by plant-soil interactions and the cost of nitrogen acquisition. *New Phytologist*, 217(2), 507–522. doi: 10.1111/nph.14872

Treseder, K.K. (2013). The extent of mycorrhizal colonization of roots and its influence on plant growth and phosphorus content. *Plant and Soil*, 371(1-2), 1–13. doi: 10.1007/s11104-013-1681-5

van Aarle, I.M., Olsson, P.A., & Soderstrom, B. (2002). Arbuscular mycorrhizal fungi respond to the substrate pH of their extraradical mycelium by altered growth and root colonization. *New Phytologist*, 155(1), 173–182. doi: 10.1046/j.1469-8137.2002.00439.x

van Aarle, I.M., & Olsson, P.A. (2003). Fungal lipid accumulation and development of mycelial structures by two arbuscular mycorrhizal fungi. *Applied and Environmental Microbiology*, 69(11), 6762–6767. doi: 10.1128/AEM.69.11.6762-6767.2003

Ven, A., Verlinden, M., Verbruggen, E., & Vicca, S. (2019). Data from: Experimental evidence that phosphorus fertilization and arbuscular mycorrhizal symbiosis can reduce the carbon cost of phosphorus uptake. doi.org/10.5281/zenodo.3387198

Verlinden, M.S., Ven, A., Verbruggen, E., Janssens, I.A., Wallander, H., & Vicca, S. (2018). Favorable effect of mycorrhizae on biomass production efficiency exceeds their carbon costs in fertilization experiment. *Ecology*, 99(11), 2525–2534. doi: 10.1002/ecy.2502

Vicca, S., Zavalloni, C., Fu, Y.S.H., Voets, L., Dupré de Boulois, H., Declerck, S., … Nijs, I. (2009). Arbuscular mycorrhizal fungi may mitigate the influence of a joint rise of

642 temperature and atmospheric CO2 on soil respiration in grasslands. *International Journal of*
643 *Ecology*, 10 pages. doi:10.1155/2009/209768
644 **Vicca, S., Luyssaert, S., Penuelas, J., Campioli, M., Chapin, F.S., Ciais, P., … Janssens,**
645 **I.A. (2012).** Fertile forests produce biomass more efficiently. *Ecology Letters*, 15(6), 520–526.
646 doi: 10.1111/j.1461-0248.2012.01775.x
647 **Vicca, S., Stocker, B., Reed, S., Wieder, W.R., Bahn, M., Fay, P., … Ciais, P. (2018).** Using
648 research networks to creaste the comprehensive datasets needed to assess nutrient availability
649 as a key determinant of terrestrial carbon cycling. *Environmental Research Letters*, 13. doi:
650 10.1088/1748-9326/aaeae7
651 **Walinga, I., van Vark, W., Houba, V.J.G., & van der Lee, J.J. (1989).** Soil and Plant
652 Analysis, Part 7. In: *Plant analysis procedures*. Agricultural University, Wageningen, 13–16.
653 **Wilson, G.W.T., & Hartnett, D.C. (1998).** Interspecific variation in plant responses to
654 mycorrhizal colonization in tallgrass prairie. *Americal Journal of Botany*, 85(12), 1732–1738.
655 **Yu, Z.H., Li, Y.S., Jin, J., Liu, X.B., & Wang, G.H. (2017).** Carbon flow in the plant-soil-
656 microbe continuum at different growth stages of maize grown in a Mollisol. *Archives of*
657 *Agronomy and Soil Science*, 63(3), 362–374. doi: 10.1080/03650340.2016.1211788

VIII. SUPPORTING INFORMATION (SI)

Appendix S1: In brief, hyphal extraction from mesh bag sand following the approach of Rillig, Field & Allen (1999)

Appendix S2: In brief, determining fatty acid methyl ester (FAME) concentrations, following the protocol of Frostegard, Tunlid & Baath (1993).

Table S3: Means and standard error (SE) of arbuscular mycorrhizal fungi (AMF) 16:1ω5 neutral lipid fatty acid (NLFA), 16:1ω5 phospholipid fatty acid (PLFA) and NLFA:PLFA ratio 37 days after planting for each phosphorus (P) fertilization treatment.

Table S4: Mean and standard error (SE) of cumulated rhizosphere respiration ($\sum R_{rhizo}$) calculated with and without $R_{rhizo} = 0$ added in dataset.

Figure S5: Observed (black circles) and predicted (grey triangles) rhizosphere respiration (R_{rhizo}) (µmol m^{-2} s^{-1}) in time (days since planting) for each phosphorus (P) fertilization treatment; R^2 value reflects the goodness of fit for observed vs. predicted.

Figure S6: Principal Component Analysis (PCA) of all variables used in analyses: aboveground biomass production, total biomass production, root biomass production, total belowground carbon flux (TBCF), rhizosphere respiration, PLFA 16:1w5, NLFA 16:1w5, and C cost of P acquisition. Colored circles refer to different treatments.

Table S7: Means and standard error (SE) of leaf, stem, root and cob nitrogen (N) and phosphorus (P) at harvest.

Please note: Wiley Blackwell are not responsible for the content or functionality of any supporting information supplied by the authors. Any queries (other than missing material) should be directed to the corresponding author for the article.

682 # IX. TABLES

683 *Table 1: Seasonal means and standard error (SE) of plant biomass carbon (C), plant phosphorus (P) and nitrogen (N) content, and PRS™-probe*

684 *nutrient supply rate in July;* BP_{above} *is aboveground biomass production,* BP_{root} *is root biomass production; root:shoot ratio calculated as* BP_{root}*:*

685 BP_{above}.

686

soil pasteurization	Number of mesocosms used in analyses (n)	treatment (P fertilization)	plant biomass carbon at harvest						plant nutrient content at harvest						PRS(tm)-probe nutrient supply rate in July					
			BP_{above}		BP_{root}		root:shoot ratio		total P (P_{tot})		total N (N_{tot})		N:P		P		NO_3-N		NH_4-N	
		($kg\ ha^{-1}$)	($g\ m^{-2}$)		($g\ m^{-2}$)		($g\ g^{-1}$)		($g\ m^{-2}$)		($g\ m^{-3}$)		($g\ g^{-1}$)		($\mu g\ cm^{-2}\ week^{-1}$)		($\mu g\ cm^{-2}\ week^{-1}$)		($\mu g\ cm^{-2}\ week^{-1}$)	
			mean	SE	mean	SE	mean	SE	mean	SE	mean	SE	mean	SE	mean	SE	mean	SE	mean	SE
unpasteurized, AMF inoculated	5	P1 (2.5)	37.69	3.83	10.60	1.92	0.29	0.06	0.19	0.02	1.98	0.17	10.49	0.41	0.049	0.010	23.246	1.656	0.482	0.085
	4 †	P2 (5)	41.05	1.33	14.07	1.28	0.34	0.03	0.21	< 0.01	2.20	0.08	10.66	0.44	0.100	0.005	25.702	2.426	0.553	0.145
	5	P3 (10)	148.20	9.66	20.87	3.43	0.14	0.02	0.76	0.04	6.86	0.41	9.03	0.31	0.218	0.020	17.462	1.041	0.640	0.124
	5	P4 (20)	179.15	6.46	23.25	2.31	0.13	0.01	1.05	0.11	8.38	0.40	8.25	0.65	0.482	0.105	19.463	1.540	0.807	0.163
pasteurized	0 ‡	P1 (2.5)	1.82	0.15	0.20	0.03	0.11	0.02	< 0.01	< 0.01	0.17	0.01	43.06	0.68	0.050	0.006	16.620	1.649	1.230	0.045
	5	P4 (20)	79.78	7.39	13.12	1.06	0.17	0.02	0.20	0.02	4.09	0.38	20.37	1.33	0.702	0.125	15.274	1.673	0.922	0.114
p-value		P fertilization	**p < 0.01**		**p < 0.01**		**p < 0.01**		**p < 0.01**		**p < 0.01**		**p < 0.01**		**p < 0.01**		p = 0.06		p = 0.08	
		pasteurization P4	**p < 0.01**		**p = 0.01**		p = 0.10		**p < 0.01**		**p < 0.01**		**p < 0.01**		p = 0.21		p = 0.15		p = 0.59	

687 *Footnotes:*

688 † *One P2 mesocosm was an outlier for aboveground biomass production (*BP_{above}*) and was therefore excluded from the analyses*

689 ‡ *All P1_noAMF plants died prematurely and were therefore excluded from the carbon partitioning analyses.*

690 **X. FIGURES**

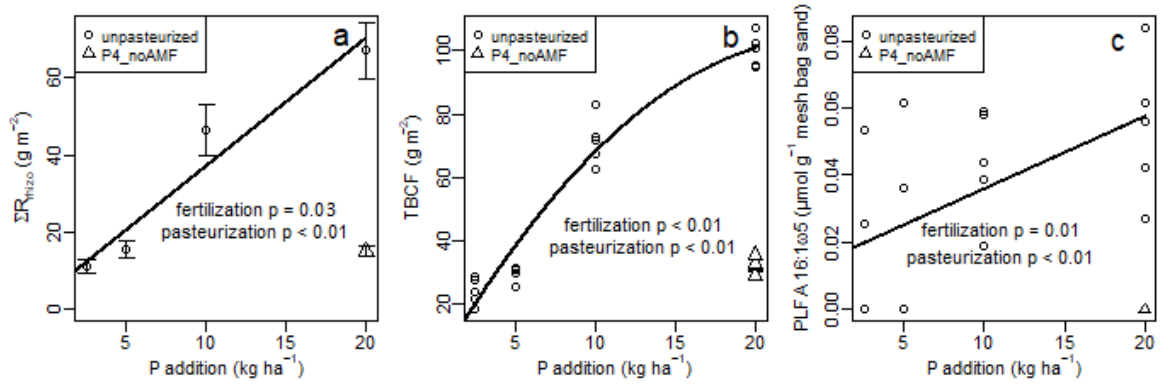

691

692 *Fig. 1: The response of cumulated rhizosphere respiration ($\sum R_{rhizo}$) (g m^{-2}) (**a**), total*
693 *belowground carbon flux (TBCF) (g m^{-2}) (**b**) and 16:1ω5 PLFA (µmol g^{-1} mesh bag sand) (**c**)*
694 *to P addition levels (kg ha^{-1}) for unpasteurized (o) and P4_noAMF (Δ) mesocosms; lines*
695 *represent relation of **a** (linear), **b** (quadratic) and **c** (linear) with P addition levels in*
696 *unpasteurized plots; p values for the main effects of P addition level and pasteurization are*
697 *provided for **a**, **b** and **c**; barplots in **a** show standard error (SE).*

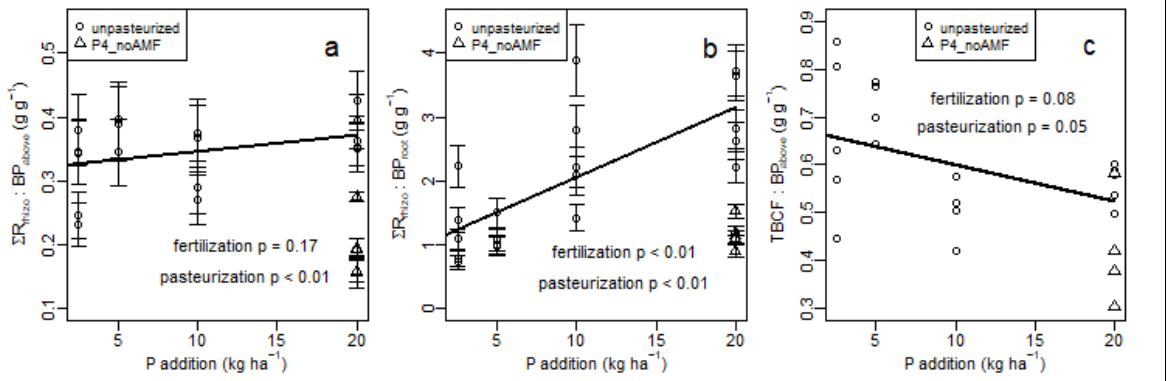

*Fig. 2: Cumulated rhizosphere respiration ($\sum R_{rhizo}$) relative to aboveground biomass production (BP_{above}) (g g^{-1}) (**a**), $\sum R_{rhizo}$ relative to root biomass production (BP_{root}) (g g^{-1}) (**b**), and total belowground biomass flux (TBCF) relative to BP_{above} (g g^{-1}) (**c**) on phosphorus (P) gradient (kg ha^{-1}) for unpasteurized (o) and P4_noAMF (Δ) mesocosms; lines represent linear relation of **a**, **b** and **c** with P addition levels in unpasteurized plots; barplots in **a** and **b** show standard error (SE); p values for the overall effects of P fertilization and pasteurization are provided for **a**, **b** and **c**.*

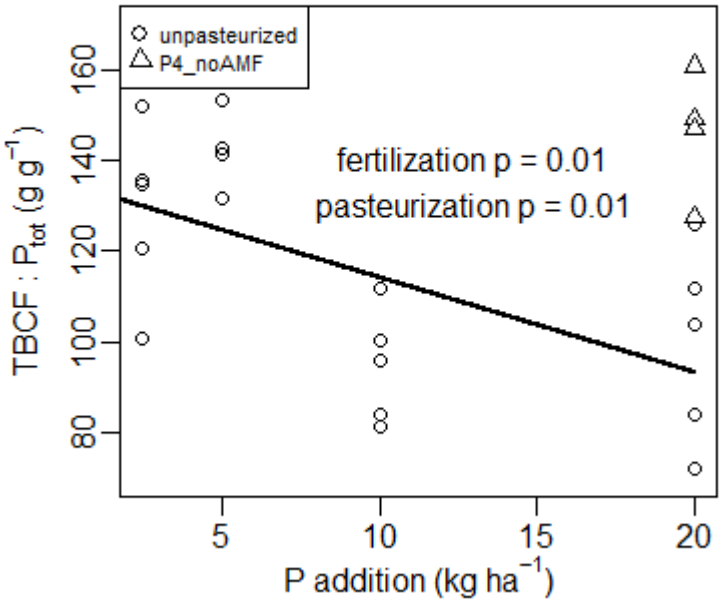

706

707 *Fig. 3: Total belowground carbon flux (TBCF) (g m^{-2}) relative to total plant phosphorus (P_{tot})*

708 *(g m^{-2}) on phosphorus (P) gradient (kg ha^{-1}) for unpasteurized (o) and P4_noAMF (Δ)*

709 *mesocosms; line represent linear relation with P addition levels in unpasteurized plots; p*

710 *values for the overall effects of P fertilization and pasteurization are provided.*

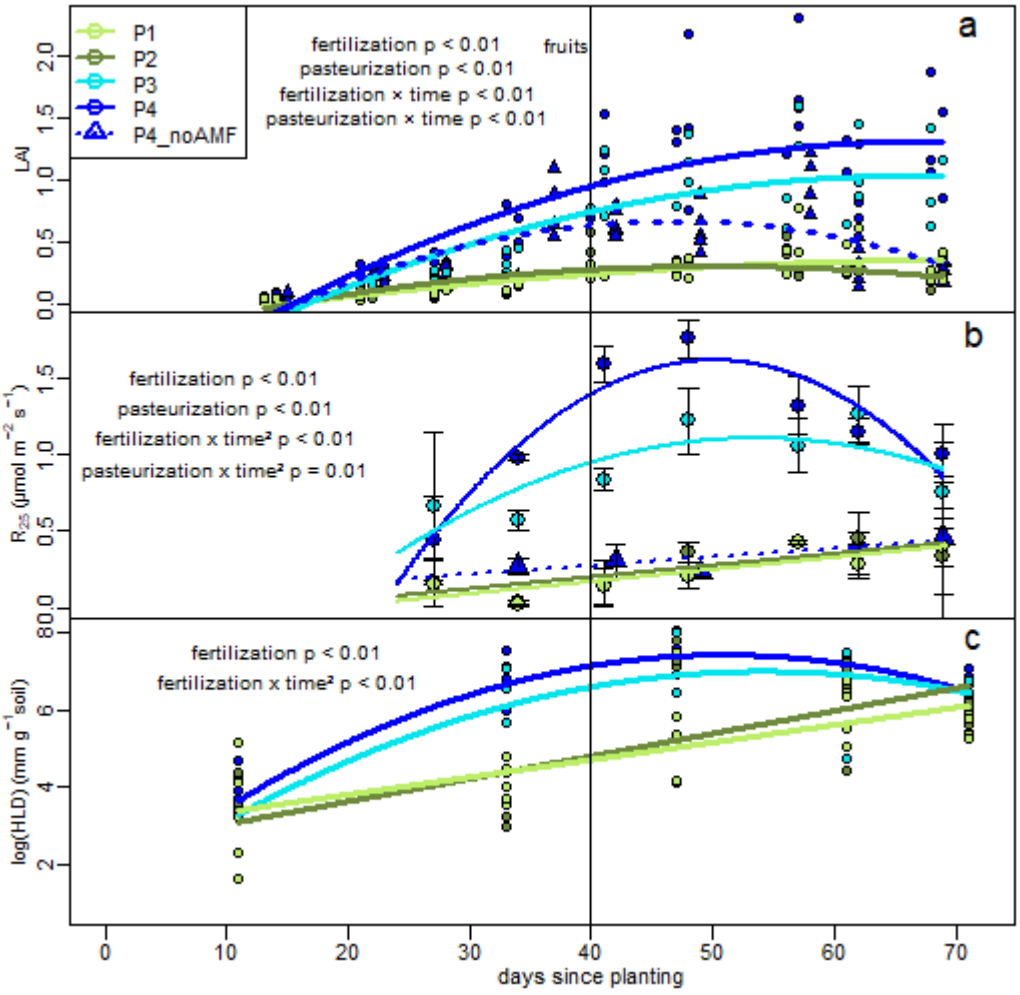

*Fig. 4: Leaf area index (LAI) (**a**),* R_{25} *(µmol* CO_2 m^{-2} s^{-1}*) (**b**), and hyphal length density (HLD) log(mm hyphae* g^{-1} *soil) (**c**) for each phosphorus-fertilizing treatment (P1 , P2, P3 and P4, respectively light green, dark green, light blue and dark blue balls and full lines) and pasteurized P4 (P4_noAMF, dark blue triangles and dotted line); lines are quadratic or linear relations with P addition levels; barplots in **b** show standard error (SE); significance for lines in **a**: P1 (p<0.01), P2 (p=0.03), P3 (p=0.13), P4 (p=0.13), P4_noAMF (p<0.01); significance for lines in **b**: P1 (p=0.02), P2 (p=0.01), P3 (p=0.06), P4 (p=0.01), P4_noAMF (p=0.07); significance for lines in **c**: P1 (p=0.01), P2 (p=0.01), P3 (p=0.01), P4 (p=0.01); p values for the overall effects of phosphorus (P) fertilization, pasteurization and their interaction with time are provided. Vertical line shows start development of fruits.*

SUPPORTING INFORMATION (SI)

Appendix S1: In brief, hyphal extraction from mesh bag sand following the approach of Rillig, Field & Allen (1999)

4 g of sand samples were suspended in 100 mL of deionized water and 12 mL of a 35 g l^{-1} sodium hexa-metaphosphate solution. In our case, the suspension was not additionally sieved because of absence of clay particles in our mesh bag sand. After the prescribed shaking and resting sequence (see Rillig *et al.*, 1999), a 10 mL aliquot was taken at 12 cm depth in an Erlenmeyer flask and pipetted onto a 25 mm diameter and 0.45 µm pore size cellulose nitrate filters (Sartorius Biolab Producs, Sartorius-Stedim Biotech). This filter was mounted to a vacuum system allowing liquids to pass through the filter, after which Sheaffer Black Ink solution (10% ink + 9% acetic acid) was used to stain the aliquot for 3 min on the filter. After removal of ink (using the vacuum pump), the filter was rinsed twice with deionized water in the same manner and transferred to a microscope slide.

Hyphal intersects were counted at 40 × 10 times magnification using a grid inside the microscope ocular at 25 locations on the filter. Hyphal length density (HLD) was calculated using equation 1 (Rillig *et al.*, 1999; Tennant, 1975):

$$HLD = (\pi * n_{int} * A * D)\,(H * W)^{-1}, \qquad \text{(eq. S1)}$$

with HLD = hyphal length density (mm hyphae g^{-1} soil), n_{int} = number of intersects where AMF hyphae were present, A = area of filter (mm^2) that was examined, D = dilution factor, H = total length of raster lines projected on filter (mm), and W = soil weight (g).

745 *Appendix S2: In brief, determining fatty acid methyl ester (FAME) concentrations, following*
746 *the protocol of Frostegard, Tunlid & Baath (1993).*
747
748 Lipids contained in 10 g sand from mesh bags harvested 47 days after planting (moment of
749 maximum HLD) were extracted for phospholipid fatty acid (PLFA) and neutral lipid fatty acid
750 (NLFA) analysis. We followed the protocol of Frostegard, Tunlid & Baath (1993), which uses
751 a one-phase mixture of chloroform, methanol and citrate buffer, and separated PLFAs (in the
752 methanol fraction) and NLFAs (in the chloroform fraction) on a silica acid column (van Aarle
753 & Olsson, 2003). These extracts were subjected to mild alkaline methanolysis and the resulting
754 FAMEs were analysed on a gas chromatograph with a flame ionization detector and a 50-m
755 HP5 capillary column using FAME 19:0 as an internal standard (Frostegard *et al*., 1993).

Table S3: Means and standard error (SE) of arbuscular mycorrhizal fungi (AMF) 16:1ω5 neutral lipid fatty acid (NLFA), 16:1ω5 phospholipid fatty acid (PLFA) and NLFA:PLFA ratio 37 days after planting for each phosphorus (P) fertilization treatment.

P fertilization	NLFA 16:1ω5		PLFA 16:1ω5		NLFA:PLFA ratio	
	nmol g^{-1} soil		nmol g^{-1} soil			
	mean	SE	mean	SE	mean	SE
P1	0.173	0.079	0.016	0.011	3.388	3.388
P2	0.698	0.197	0.039	0.015	17.137	2.061
P3	0.481	0.173	0.044	0.007	14.745	2.507
P4	0.722	0.219	0.054	0.010	10.906	1.783
P1_noAMF and P4_noAMF	0	0	0	0	0	0

760 *Table S4: Mean and standard error (SE) of cumulated rhizosphere respiration ($\sum R_{rhizo}$)*
761 *calculated with and without R_{rhizo} = 0 added in dataset.*

pasteurization	treatment (P fertilization)	$\sum R_{rhizo}$					
	(kg ha^{-1})	(g m^{-2})					
		R_{rhizo} = 0 added			no R_{rhizo} = 0 added		
		mean	SE	R^2 value	mean	SE	R^2 value
unpasteurized	P1 (2.5)	11.2053	1.6392	0.9975	10.3838	1.5095	0.9927
	P2 (5)	12.737	2.3243	0.9993	14.19995	2.1134	0.9973
	P3 (10)	46.3409	6.6383	0.9957	41.073	5.8131	0.9918
	P4 (20)	67.146	7.2859	0.9942	57.6123	6.1785	0.9886
pasteurized	P1_noAMF (2.5)	3.2085	0.3161	0.9857	1.6833	0.1647	0.9301
	P4_noAMF (20)	15.0163	1.3737	0.9941	16.5054	1.5102	0.9967

762

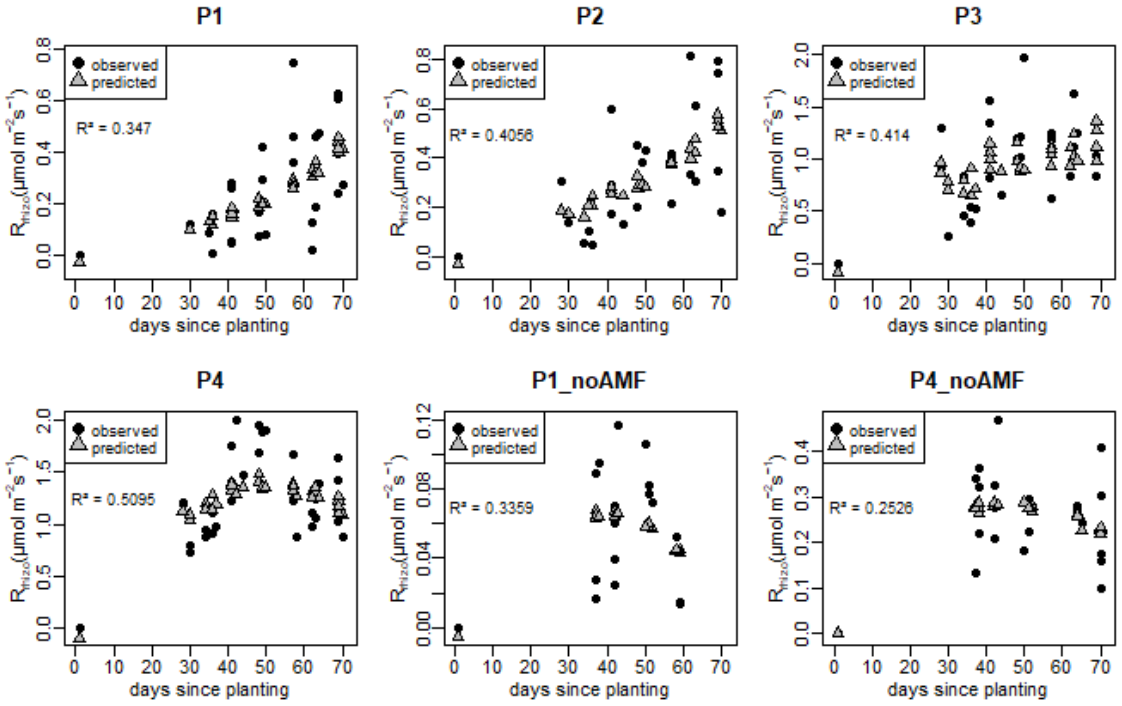

763

764 *Figure S5: Observed (black circles) and predicted (grey triangles) rhizosphere respiration*
765 *(R_{rhizo}) (µmol m^{-2} s^{-1}) in time (days since planting) for each phosphorus (P) fertilization*
766 *treatment; R^2 value reflects the goodness of fit for observed vs. predicted.*

767

768 *Footnote: for the model we used, the residuals of observed vs. predicted were not normally*
769 *distributed in P4 (W = 0.80), P1_noAMF (W = 0.84) and P4_noAMF (W = 0.84). However,*
770 *R^2 in P4 was highest of all treatments and an underestimation of predicted R_{rhizo} in P4,*
771 *P4_noAMF or P1_noAMF cannot lead to divergent interpretations since they were clearly*
772 *differing with other treatments. Results of P1_noAMF were not used in the paper.*

773

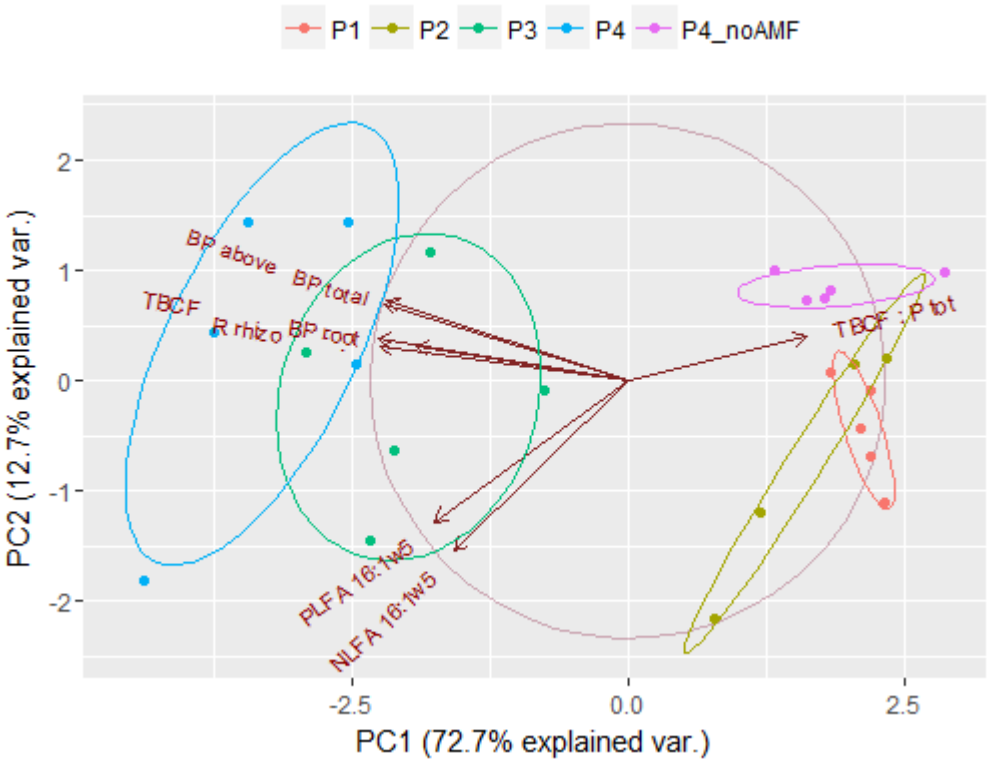

774

775 *Figure S6: Principal Component Analysis (PCA) of all variables used in analyses:*
776 *aboveground biomass production (BP above), total biomass production (BP total), root*
777 *biomass production (BP root), total belowground carbon flux (TBCF), rhizosphere respiration*
778 *(R rhizo), PLFA 16:1w5, NLFA 16:1w5, and C cost of P acquisition (TBCF : P tot). Coloured*
779 *circles refer to different treatments.*

780

781 The PCA indicates a tight coupling between aboveground and total biomass production, root
782 biomass production, rhizosphere respiration and TBCF across the treatments. The opposite
783 direction for the C cost of P acquisition illustrates the increasing C cost with decreasing nutrient
784 availability and with pasteurization. The P gradient, and especially the difference between P1,
785 P2 vs P3, P4 clearly emerges in PC1. Also in PC1, pasteurization seems to have pushed the
786 high P mesocosms towards the low P mesocosms.

787 *Table S7: Means and standard error (SE) of leaf, stem, root and cob nitrogen (N) and phosphorus (P) at harvest.*

treatment		plant part																			
pasteurization	P fertilization	leaf										stem									
		[P]		total P		[N]		total N		N:P		[P]		total P		[N]		total N		N:P	
	(kg ha^{-1})	g kg^{-1} biomass		g m^{-2}		g kg^{-1} biomass		g m^{-2}		g g^{-1}		g kg^{-1} biomass		g m^{-2}		g kg^{-1} biomass		g m^{-2}		g g^{-1}	
		mean	SE	mean	SE	mean	SE	mean	SE	mean	SE	mean	SE	mean	SE	mean	SE	mean	SE	mean	SE
unpasteurized	P1 (2.5)	1.831	0.064	0.026	0.003	28.789	0.366	0.420	0.054	15.789	0.521	0.679	0.037	0.017	0.002	9.515	0.336	0.243	0.028	14.101	0.494
	P2 (5)	1.762	0.139	0.026	0.003	28.364	0.951	0.421	0.026	16.295	0.877	0.714	0.075	0.020	0.002	10.554	0.630	0.300	0.018	15.047	0.969
	P3 (10)	1.823	0.084	0.088	0.003	25.906	0.353	1.263	0.059	14.308	0.567	0.621	0.057	0.058	0.003	9.087	0.579	0.859	0.062	14.871	0.884
	P4 (20)	1.542	0.087	0.093	0.009	23.369	0.350	1.398	0.070	15.353	0.906	0.597	0.044	0.070	0.006	10.260	1.000	1.193	0.121	17.095	0.539
pasteurized	P1_noAMF (2.5)	0.764	0.004	0.002	0.000	35.264	0.748	0.110	0.004	46.183	0.959	0.859	0.042	0.001	0.000	34.303	2.215	0.048	0.012	39.925	1.343
	P4_noAMF (20)	0.697	0.023	0.022	0.002	22.340	0.687	0.711	0.054	32.179	1.290	0.321	0.023	0.021	0.003	12.664	1.145	0.861	0.152	40.308	4.721
value ANCOVA	P fertilization	**p=0.03**		**p<0.01**		**p<0.01**		**p<0.01**		p=0.48		p=0.15		**p<0.01**		p=0.68		**p<0.01**		**p<0.01**	
	pasteurization P4	**p<0.01**		**p<0.01**		p=0.22		**p<0.01**		**p<0.01**		**p<0.01**		**p<0.01**		p=0.15		p=0.13		**p<0.01**	

treatment		plant part																			
pasteurization	P fertilization	root										cob									
		[P]		total P		[N]		total N		N:P		[P]		total P		[N]		total N		N:P	
	(kg ha^{-1})	g kg^{-1} biomass		g m^{-2}		g kg^{-1} biomass		g m^{-2}		g g^{-1}		g kg^{-1} biomass		g m^{-2}		g kg^{-1} biomass		g m^{-2}		g g^{-1}	
		mean	SE	mean	SE	mean	SE	mean	SE	mean	SE	mean	SE	mean	SE	mean	SE	mean	SE	mean	SE
unpasteurized	P1 (2.5)	0.563	0.029	0.017	0.003	10.122	0.510	0.296	0.045	18.081	0.920	2.535	0.135	0.129	0.012	19.991	0.435	1.017	0.084	7.970	0.438
	P2 (5)	0.535	0.018	0.021	0.002	9.357	0.245	0.375	0.033	17.525	0.284	2.489	0.053	0.139	0.002	19.741	0.800	1.111	0.072	7.959	0.461
	P3 (10)	0.705	0.054	0.042	0.008	9.884	0.257	0.583	0.089	14.314	0.991	2.700	0.182	0.573	0.042	19.488	0.442	4.159	0.281	7.306	0.339
	P4 (20)	0.647	0.056	0.043	0.006	10.024	0.614	0.663	0.069	15.807	1.158	3.305	0.489	0.844	0.118	20.062	1.041	5.130	0.258	6.391	0.578
pasteurized	P1_noAMF (2.5)	0.519	0.048	0.000	0.000	14.441	1.258	0.008	0.001	27.896	0.722	0.000	0.000	0.000	0.000	0.000	0.000	0.000	0.000	0.000	0.000
	P4_noAMF (20)	0.392	0.017	0.015	0.001	11.426	0.730	0.430	0.054	29.518	2.668	1.446	0.032	0.146	0.017	20.997	0.409	2.091	0.203	14.575	0.595
value ANCOVA	P fertilization	p=0.12		**p<0.01**		p=0.77		**p<0.01**		p=0.11		**p=0.03**		**p<0.01**		p=0.87		**p<0.01**		**p<0.01**	
	pasteurization P4	**p<0.01**		**p<0.01**		p=0.18		**p=0.03**		**p<0.01**		**p=0.01**		**p<0.01**		p=0.43		**p<0.01**		**p<0.01**	

788

SUPPORTING INFORMATION (SI)

Additional supporting information may be found in the online version of this article.

Appendix S1: In brief, hyphal extraction from mesh bag sand following the approach of Rillig, Field & Allen (1999)

4 g of sand samples were suspended in 100 mL of deionized water and 12 mL of a 35 g l^{-1} sodium hexa-metaphosphate solution. In our case, the suspension was not additionally sieved because of absence of clay particles in our mesh bag sand. After the prescribed shaking and resting sequence (see Rillig *et al.*, 1999), a 10 mL aliquot was taken at 12 cm depth in an Erlenmeyer flask and pipetted onto a 25 mm diameter and 0.45 µm pore size cellulose nitrate filters (Sartorius Biolab Producs, Sartorius-Stedim Biotech). This filter was mounted to a vacuum system allowing liquids to pass through the filter, after which Sheaffer Black Ink solution (10% ink + 9% acetic acid) was used to stain the aliquot for 3 min on the filter. After removal of ink (using the vacuum pump), the filter was rinsed twice with deionized water in the same manner and transferred to a microscope slide.

Hyphal intersects were counted at 40 × 10 times magnification using a grid inside the microscope ocular at 25 locations on the filter. Hyphal length density (HLD) was calculated using equation 1 (Rillig *et al.*, 1999; Tennant, 1975):

$$HLD = (\pi * n_{int} * A * D) (H * W)^{-1}, \quad \text{(eq. S1)}$$

with HLD = hyphal length density (mm hyphae g^{-1} soil), n_{int} = number of intersects where AMF hyphae were present, A = area of filter (mm^2) that was examined, D = dilution factor, H = total length of raster lines projected on filter (mm), and W = soil weight (g).

818 *Appendix S2: In brief, determining fatty acid methyl ester (FAME) concentrations, following*
819 *the protocol of Frostegard, Tunlid & Baath (1993).*
820
821 Lipids contained in 10 g sand from mesh bags harvested 47 days after planting (moment of
822 maximum HLD) were extracted for phospholipid fatty acid (PLFA) and neutral lipid fatty acid
823 (NLFA) analysis. We followed the protocol of Frostegard, Tunlid & Baath (1993), which uses
824 a one-phase mixture of chloroform, methanol and citrate buffer, and separated PLFAs (in the
825 methanol fraction) and NLFAs (in the chloroform fraction) on a silica acid column (van Aarle
826 & Olsson, 2003). These extracts were subjected to mild alkaline methanolysis and the resulting
827 FAMEs were analysed on a gas chromatograph with a flame ionization detector and a 50-m
828 HP5 capillary column using FAME 19:0 as an internal standard (Frostegard *et al*., 1993).

Table S3: Means and standard error (SE) of arbuscular mycorrhizal fungi (AMF) 16:1ω5 neutral lipid fatty acid (NLFA), 16:1ω5 phospholipid fatty acid (PLFA) and NLFA:PLFA ratio 37 days after planting for each phosphorus (P) fertilization treatment.

P fertilization	NLFA 16:1ω5		PLFA 16:1ω5		NLFA:PLFA ratio	
	nmol g^{-1} soil		nmol g^{-1} soil			
	mean	SE	mean	SE	mean	SE
P1	0.173	0.079	0.016	0.011	3.388	3.388
P2	0.698	0.197	0.039	0.015	17.137	2.061
P3	0.481	0.173	0.044	0.007	14.745	2.507
P4	0.722	0.219	0.054	0.010	10.906	1.783
P1_noAMF and P4_noAMF	0	0	0	0	0	0

833 *Table S4: Mean and standard error (SE) of cumulated rhizosphere respiration ($\sum R_{rhizo}$)*
834 *calculated with and without R_{rhizo} = 0 added in dataset.*

pasteurization	treatment (P fertilization)	$\sum R_{rhizo}$					
	(kg ha^{-1})	(g m^{-2})					
		R_{rhizo} = 0 added			no R_{rhizo} = 0 added		
		mean	SE	R^2 value	mean	SE	R^2 value
unpasteurized	P1 (2.5)	11.2053	1.6392	0.9975	10.3838	1.5095	0.9927
	P2 (5)	12.737	2.3243	0.9993	14.19995	2.1134	0.9973
	P3 (10)	46.3409	6.6383	0.9957	41.073	5.8131	0.9918
	P4 (20)	67.146	7.2859	0.9942	57.6123	6.1785	0.9886
pasteurized	P1_noAMF (2.5)	3.2085	0.3161	0.9857	1.6833	0.1647	0.9301
	P4_noAMF (20)	15.0163	1.3737	0.9941	16.5054	1.5102	0.9967

835

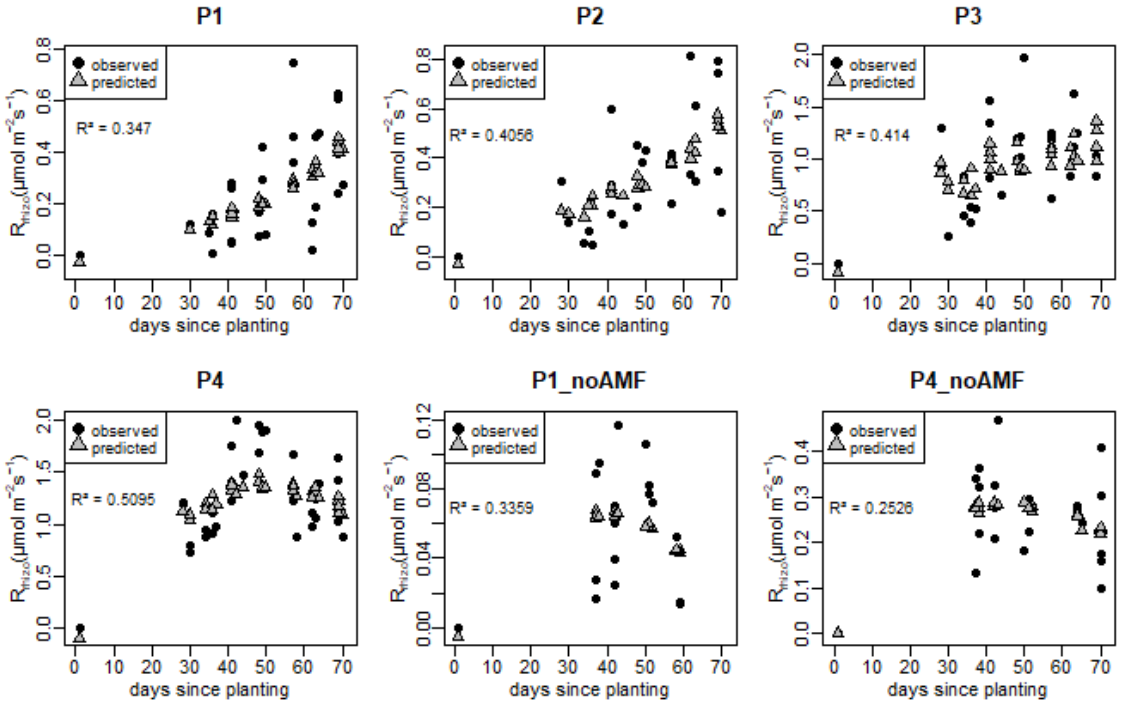

Figure S5: Observed (black circles) and predicted (grey triangles) rhizosphere respiration (R_{rhizo}) (µmol m^{-2} s^{-1}) in time (days since planting) for each phosphorus (P) fertilization treatment; R^2 value reflects the goodness of fit for observed vs. predicted.

Footnote: for the model we used, the residuals of observed vs. predicted were not normally distributed in P4 (W = 0.80), P1_noAMF (W = 0.84) and P4_noAMF (W = 0.84). However, R^2 in P4 was highest of all treatments and an underestimation of predicted R_{rhizo} in P4, P4_noAMF or P1_noAMF cannot lead to divergent interpretations since they were clearly differing with other treatments. Results of P1_noAMF were not used in the paper.

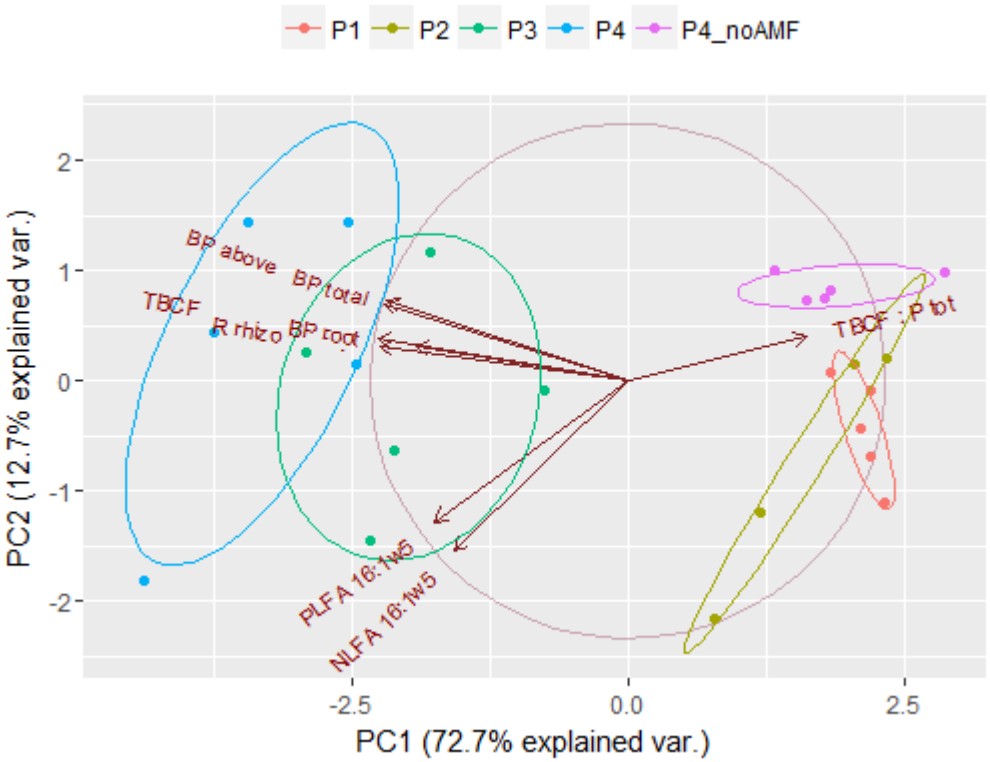

847

848 *Figure S6: Principal Component Analysis (PCA) of all variables used in analyses:*
849 *aboveground biomass production (BP above), total biomass production (BP total), root*
850 *biomass production (BP root), total belowground carbon flux (TBCF), rhizosphere respiration*
851 *(R rhizo), PLFA 16:1w5, NLFA 16:1w5, and C cost of P acquisition (TBCF : P tot). Coloured*
852 *circles refer to different treatments.*

853

854 The PCA indicates a tight coupling between aboveground and total biomass production, root
855 biomass production, rhizosphere respiration and TBCF across the treatments. The opposite
856 direction for the C cost of P acquisition illustrates the increasing C cost with decreasing nutrient
857 availability and with pasteurization. The P gradient, and especially the difference between P1,
858 P2 vs P3, P4 clearly emerges in PC1. Also in PC1, pasteurization seems to have pushed the
859 high P mesocosms towards the low P mesocosms.

860 *Table S7: Means and standard error (SE) of leaf, stem, root and cob nitrogen (N) and phosphorus (P) at harvest.*

treatment		plant part																			
pasteurization	P fertilization	leaf										stem									
		[P]		total P		[N]		total N		N:P		[P]		total P		[N]		total N		N:P	
	(kg ha^{-1})	g kg^{-1} biomass		g m^{-2}		g kg^{-1} biomass		g m^{-2}		g g^{-1}		g kg^{-1} biomass		g m^{-2}		g kg^{-1} biomass		g m^{-2}		g g^{-1}	
		mean	SE	mean	SE	mean	SE	mean	SE	mean	SE	mean	SE	mean	SE	mean	SE	mean	SE	mean	SE
unpasteurized	P1 (2.5)	1.831	0.064	0.026	0.003	28.789	0.366	0.420	0.054	15.789	0.521	0.679	0.037	0.017	0.002	9.515	0.336	0.243	0.028	14.101	0.494
	P2 (5)	1.762	0.139	0.026	0.003	28.364	0.951	0.421	0.026	16.295	0.877	0.714	0.075	0.020	0.002	10.554	0.630	0.300	0.018	15.047	0.969
	P3 (10)	1.823	0.084	0.088	0.003	25.906	0.353	1.263	0.059	14.308	0.567	0.621	0.057	0.058	0.003	9.087	0.579	0.859	0.062	14.871	0.884
	P4 (20)	1.542	0.087	0.093	0.009	23.369	0.350	1.398	0.070	15.353	0.906	0.597	0.044	0.070	0.006	10.260	1.000	1.193	0.121	17.095	0.539
pasteurized	P1_noAMF (2.5)	0.764	0.004	0.002	0.000	35.264	0.748	0.110	0.004	46.183	0.959	0.859	0.042	0.001	0.000	34.303	2.215	0.048	0.012	39.925	1.343
	P4_noAMF (20)	0.697	0.023	0.022	0.002	22.340	0.687	0.711	0.054	32.179	1.290	0.321	0.023	0.021	0.003	12.664	1.145	0.861	0.152	40.308	4.721
value ANCOVA	P fertilization	**p=0.03**		**p<0.01**		**p<0.01**		**p<0.01**		p=0.48		p=0.15		**p<0.01**		p=0.68		**p<0.01**		**p<0.01**	
	pasteurization P4	**p<0.01**		**p<0.01**		p=0.22		**p<0.01**		**p<0.01**		**p<0.01**		**p<0.01**		p=0.15		p=0.13		**p<0.01**	

treatment		plant part																			
pasteurization	P fertilization	root										cob									
		[P]		total P		[N]		total N		N:P		[P]		total P		[N]		total N		N:P	
	(kg ha^{-1})	g kg^{-1} biomass		g m^{-2}		g kg^{-1} biomass		g m^{-2}		g g^{-1}		g kg^{-1} biomass		g m^{-2}		g kg^{-1} biomass		g m^{-2}		g g^{-1}	
		mean	SE	mean	SE	mean	SE	mean	SE	mean	SE	mean	SE	mean	SE	mean	SE	mean	SE	mean	SE
unpasteurized	P1 (2.5)	0.563	0.029	0.017	0.003	10.122	0.510	0.296	0.045	18.081	0.920	2.535	0.135	0.129	0.012	19.991	0.435	1.017	0.084	7.970	0.438
	P2 (5)	0.535	0.018	0.021	0.002	9.357	0.245	0.375	0.033	17.525	0.284	2.489	0.053	0.139	0.002	19.741	0.800	1.111	0.072	7.959	0.461
	P3 (10)	0.705	0.054	0.042	0.008	9.884	0.257	0.583	0.089	14.314	0.991	2.700	0.182	0.573	0.042	19.488	0.442	4.159	0.281	7.306	0.339
	P4 (20)	0.647	0.056	0.043	0.006	10.024	0.614	0.663	0.069	15.807	1.158	3.305	0.489	0.844	0.118	20.062	1.041	5.130	0.258	6.391	0.578
pasteurized	P1_noAMF (2.5)	0.519	0.048	0.000	0.000	14.441	1.258	0.008	0.001	27.896	0.722	0.000	0.000	0.000	0.000	0.000	0.000	0.000	0.000	0.000	0.000
	P4_noAMF (20)	0.392	0.017	0.015	0.001	11.426	0.730	0.430	0.054	29.518	2.668	1.446	0.032	0.146	0.017	20.997	0.409	2.091	0.203	14.575	0.595
value ANCOVA	P fertilization	p=0.12		**p<0.01**		p=0.77		**p<0.01**		p=0.11		**p=0.03**		**p<0.01**		p=0.87		**p<0.01**		**p<0.01**	
	pasteurization P4	**p<0.01**		**p<0.01**		p=0.18		**p=0.03**		**p<0.01**		**p=0.01**		**p<0.01**		p=0.43		**p<0.01**		**p<0.01**	

861

862 Please note: Wiley Blackwell are not responsible for the content or functionality of any
863 supporting information supplied by the authors. Any queries (other than missing material)
864 should be directed to the corresponding author for the article.

865

866